Characteristics of sand waves with groins in series

S. M. Habibullah Bahar
Hiroshima University, Higashi-Hiroshima City, Japan

S. Fukuoka
Hiroshima University, Higashi-Hiroshima City, Japan

ABSTRACT: This paper shows the characteristic changes of bedforms, equivalent roughness and more irregularities of sand waves due to the presence of the groins compared to a bed without groins, which nevertheless have the same hydraulic conditions. However, for a relatively low groin height, the groin bedform is very similar to the bed without groins. By analogy with ocean waves, a functional relationship between the area under power spectrum density function of sand waves and average bedform height is derived from the auto-correlation function of the longitudinal bed elevation. This relationship is verified from other authors, by our precise laboratory experiments and irrigation channel data. The bedform height and length follow different distribution functions; the former fitting well with Rayleigh distribution and the latter following Normal distribution.

1 INTRODUCTION

Researchers have concentrated a great deal on bedform mechanics and the geometrical structure of bedforms in alluvial channels and rivers. Most of the bedform investigations did not consider the effects of hydraulic structure on bed formation except for local scouring. Fukuoka et al. (1998) studied the bed topography around submersible and impermeable groins in series, but not the bed formation far from the groin head.

For ocean waves (Ochi, 1998), the area under the spectral density function is related to the second power of significant wave height assuming narrow-banded spectrum. Ashida et al. (1967) showed that dimensionless bedform height and bedform length fitted the Rayleigh distribution well.

The present study investigates the variation of bedforms and bedform roughness due to the presence and arrangements of hydraulic structures, such as submersible permeable and impermeable groins installed in the flume. It also explores the bed profiles by spectrum analysis. In a similar fashion to the case of ocean waves, a functional relationship is derived (Bahar, 1999) for power spectrum of bed profile and bedform height by auto-correlation function. We have verified this relationship by the other authors and our experimental and irrigation channel data. In a companion study (1999), it was shown that the distribution of bedform height and length fitted different distribution functions.

2 EXPERIMENTAL PROCEDURE

The laboratory straight flume of the mobile bed is 27.5m long and 1.5m wide. It had re-circulation of water and a continuous sediment supply with an instrument carriage moving across in the upstream of the channel during the experiments.

The total number of experiments were ten: two experiments without hydraulic structure (Case A and Case B) in the bed, six experiments with impermeable groins (Case 1 to Case 6), and two experiments with permeable groins (Case 7 and Case 8). The hydraulic conditions of one experiment without hydraulic structure (Case A) are shown in Table 1. They were the

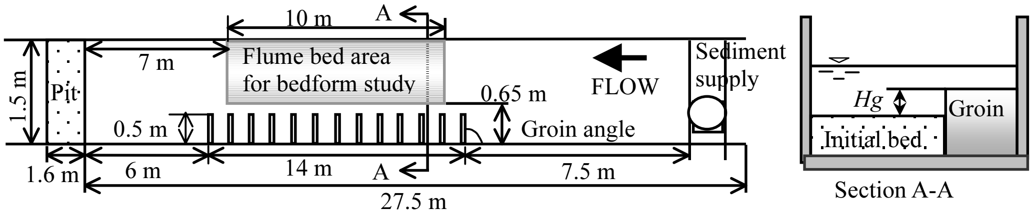

Figure 1: Experimental setup of groin experiment.

Table 1. Experimental conditions and results.

	Case 1	**Case 2**	**Case 3**	**Case 4**	**Case 5**	**Case 6**	**Case 7**	**Case 8**	**Case A**	**Case B**
Permeability	Imp.	Imp.	Imp.	Imp.	Imp.	Imp.	Per.	Per.		
Groin angle	105^0	105^0	90^0	90^0	75^0	90^0	90^0	90^0		
Gr. interval, m	1.0	0.75	0.75	1.0	1.0	1.0	1.0	1.0		
Gr. height, cm	3	3	3	3	3	2	3	5		
Water dis.,l/s	36.4									90
S. supp., l/s	0.004									0.014
W. slope x10^2	0.21	0.19	0.2	0.2	0.18	0.17	0.17	0.16	0.17	0.21
Bed slope x10^2	0.28	0.2	0.19	0.22	0.26	0.18	0.23	0.29	0.14	0.16
Flow depth, cm	10.5	8.08	8.58	7.8	8.3	7	7.3	8.2	6.47	14.4
u_*, cm/s	4.7	3.87	3.81	3.85	3.4	3.5	3.5	3.63	3.32	5.6
Bedform, H cm	2.63	1.85	2.26	1.7	2.16	1.4	1.56	1.9	1.45	4.7
Bedform, L cm	78.4	83.1	78.5	81.4	83.3	114	93.5	82.4	118	99.8
Bedform,H_0 cm	2.8	1.9	2.42	1.8	2.3	1.42	1.63	2.04	1.47	4.98
Bedform,L_0 cm	88.7	97.2	98.8	110	96.3	133	111	107	130	123
$H_{1/3}$, cm	3.84	2.7	3.4	2.6	3.2	2.1	2.2	2.83	2.3	7
σ, cm	1.3	1	1.1	0.9	0.9	0.8	0.8	1.2	0.7	2.7
Ks, cm	3	0.98	1.44	1.5	1.58	0.96	0.83	1.08	0.77	8.1

same as the groin experiments, but those of Case B were larger than with the groin experiments. The bed consisting of uniform non-cohesive sediment with the D_{50} size of 0.80mm was initially flat, having a slope in the range of 0.0018 to 0.0016.

Impermeable groin experiments were carried out with different arrangements of groins (Table 1) by intervals between two neighboring groins, groin angles from the left bank of the flume and groin height. The groin angles measured from the left bank were 75, 90 and 105 degrees. The protruded height of the groin from the initial sand bed was considered as groin height Hg (Figure 1). The groins in each experiment were arranged along the left bank (Figure 1) starting at a distance of 6m from the downstream end to 20m upstream with same interval, angle and height. Their length and width were 50cm and 5cm, respectively.

By ultra-sonic profile indicator, we measured nearly equilibrium longitudinal bed profile. For power spectrum analyses, the bed elevation Y as a function of longitudinal distance x had 71 numbers of bed elevation data.

3 COMPARATIVE STUDY OF BEDFORM

The bedforms of our experimental beds were dunes superimposed by smaller bedforms of ripples, according to the JSCE task committee, 1974. We employed two methods to identify a single sand wave unit and to measure the bedform dimensions. These are based on alternate slope change and alternate zero-crossing of mean bed level. In this paper, if not otherwise mentioned, bedform height and bedform length denotes the geometrical dimension of sand waves measured by the alternate slope change method.

The properties of sand wave based on alternate slope change method are: it has a peak that follows a steep slope, a trough in the downstream direction and a gentle slope towards the upstream direction. The distance from the trough of the sand wave to the next downstream sand wave trough is considered as the bedform length L. The difference between the elevations of the sand wave peak and the next downstream trough is estimated as the bedform height H. A sand wave based on the alternate zero-crossing method is the one that only alternately crosses the mean bed level, having positive maxima and negative maxima of bedform height. The distance between two successive crossing points by mean bed level and the steeper slope of sand wave is estimated as zero-crossing bedform length L_0.

Crickmore (1970) showed that the bedform length ratio L_0/L was larger for 3-dimensional bedforms than for 2-dimensional bedforms. In our experimental beds, the bedform length based on alternate zero-crossing varies significantly from that of alternate slope change, depending on dimensional properties of sand waves. The bedform length ratio of L_0/L varies from 1.10 to 1.35 and bedform height ratio H_0/H is 1.06. The plan view of the Case A shows sinuous and continuous sand wave peaks across the flume, which indicates nearly two-dimensional bedforms. As a result, its ratio L_0/L is lowest 1.10 of all the beds. On the other hand, the sand wave peaks of the groin experimental beds possess higher degrees of sinuosity and discontinuity across the flume. As is similar to Crickmore's observation, 3-dimensional shape and transverse irregularities of the groin bedforms cause higher ratio of L_0/L.

Case 1 impermeable groin bed has the highest bedform height and the shortest bedform length (Table 1) among the groin related experiments. On the other hand, the bedform of Case A is just the opposite of Case 1 groin bedform. Case 1 has 80% larger bedform height and 30% shorter bedform length compared to Case A. Among the impermeable groin beds with 3cm groin height, Case 4 exhibits the smallest bedform height (17% greater than Case A), even smaller than Case 2 possessing the same arrangement but 0.75m groin interval. Along with other groin parameters, groin height imparts significant influence on bedforms. Case 4 and Case 6 impermeable groins have the same arrangements except in the different groin height of 3cm and 2cm respectively. The bedform of Case 6 groin bed is not only smaller than that of Case 4 bed, but also the smallest of all the groin bedforms. Even installing groins in Case 6, its bedform is very similar to Case A. The permeability of Case 7 groin causes less undulation of bed profiles than the other impermeable groin beds (Case 1 to Case 5) of same 3cm groin height. Even possessing permeability, the bedform height and length are 8% larger and 20% shorter compared to those of Case A respectively. The larger groin height of Case 8 causes higher bedform height than that of Case 7 (30% greater bedform height and 30% shorter bedform length than Case A).

Figure 2: Groin bedform steepness.

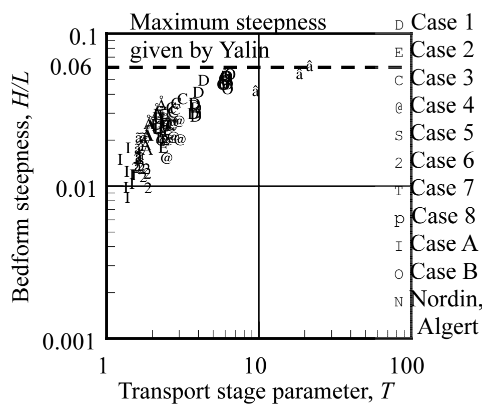

In Figure 2, bedform steepness of each longitudinal profile of all the experiments is plotted as a function of transport stage parameter or the Shields parameter $T = (u_*/u_{*c})^2 - 1$. Here, u_* is the bed shear velocity; and u_{*c} is the critical bed shear velocity. It shows the effects of the groins on bedform, where the bedform steepness increases with the increase of T of the groin beds. Similar to the case of previous bedform analyses, Case 1 groin bed displays largest transport stage parameter along with highest bedform steepness. The bedform steepness of the Case 6 bed is almost close to

Case A, and it is even less than that of Case 7 and Case 8 permeable groin beds. We have analyzed data from Nordin et al. (1966) for bedform steepness of the experimental beds. For this data, the average bedform height was estimated from the significant dune height divided by a factor of 1.5, obtained from our experimental results. The bedform steepness of Case B, bed without groin, is higher than that with the groin beds, but less than the Nordin et al. data and the maximum steepness 0.06 for dunes according to Yalin (1972). As the groin bedform steepness is even less than Case B bed and the Nordin et al. data, its steepness may further increase with an increase of tractive force or groin height.

4 STATISTICAL ANALYSIS

Nordin et al. (1966) initiated the study of statistical properties of sand waves and since then promising progress has been made by a number of researchers. The wave number spectrum density function of the bed without groin (Figure 3(a)) has a similar slope to the '-3 power law' but the proportionality factor of

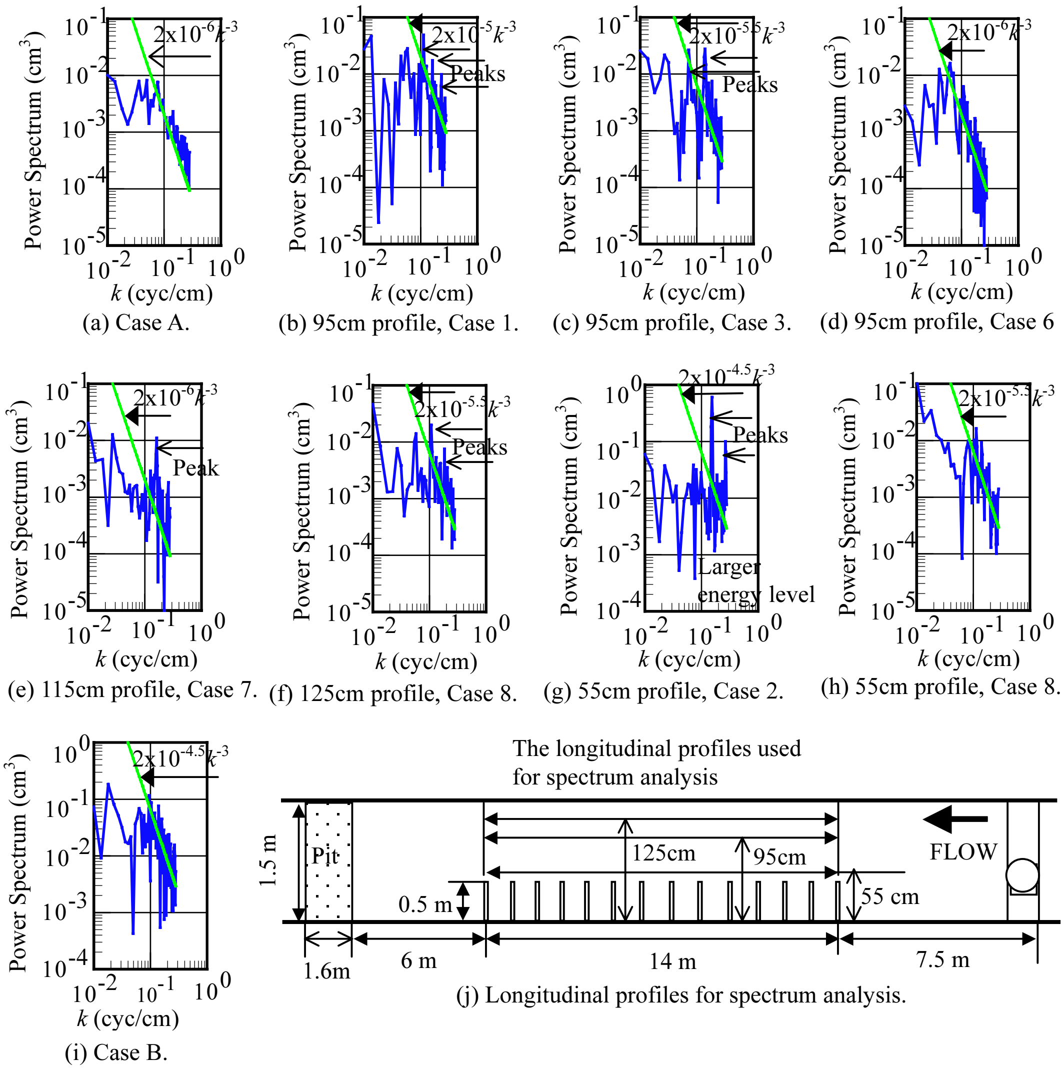

(a) Case A. (b) 95cm profile, Case 1. (c) 95cm profile, Case 3. (d) 95cm profile, Case 6

(e) 115cm profile, Case 7. (f) 125cm profile, Case 8. (g) 55cm profile, Case 2. (h) 55cm profile, Case 8.

(i) Case B. (j) Longitudinal profiles for spectrum analysis.

$2x10^{-6}$ is different from the value stated by Hino (1968). Two spectral peaks experimentally observed by Jain et al. (1974), each with different dominant wave number, were supposed to describe the physical and geometrical mechanisms of two distinct types of sand waves. The first peak might be related to the bedform of large wavelength at a lower wave number and the second peak at a higher wave number, related to the instability of an interaction between the erodible bed and the turbulent flow. Sand waves having a larger wave number will progress faster than those with a lower number. The bedforms of shorter wavelength will overtake the longer, slower moving ones being absorbed by the latter. This physical mechanism of shorter bedform movement was more prominent during the groin experiments compared to Case A bed.

The spectra of longitudinal bed profile of Case 1 and Case 3 (Figure 3(b) & 3(c)) impermeable groin beds show more than two spectral peaks at lower as well as at higher wave number. The reason is that irregularities of sand waves increased and more groups of smaller wavelength were present in the groin beds compared to Case A. The proportional factor of '-3 power law' is not constant, but it varies along with hydraulic variables. This factor for the impermeable groin beds increased by 10 times along with bed shear stress compared to bed without groins, except in Case 6. The spectrum of Case 6 (Figure 3(d)) have similar bedforms and the proportional factor of '-3 power law' to those of Case A, and neither show a large spectrum peak as the groin beds at high wave number except for local scours. A large amplitude spectral peak at high wave numbers of Case 1 and Case 3 indicates more non-equilibrium sediment transport and irregularities of sand waves than the bed without groins.

The proportional factor of '-3 power law' of Case 7 is nearly identical to Case A, but it increases by a factor of 3 for Case 8. The impermeable groin beds had deeper local scouring depth than the permeable groin beds. Similarly, spectrums along the lines near groin local scouring of impermeable groin beds (Figure 3(g)) have larger peaks, because of higher energy level, at high wave number compared to the permeable (Figure 3(h)) groin beds. Case B bed's spectrum (Figure 3(i)) follows the '-3 power law' but with a different and the largest proportional factor of all the beds.

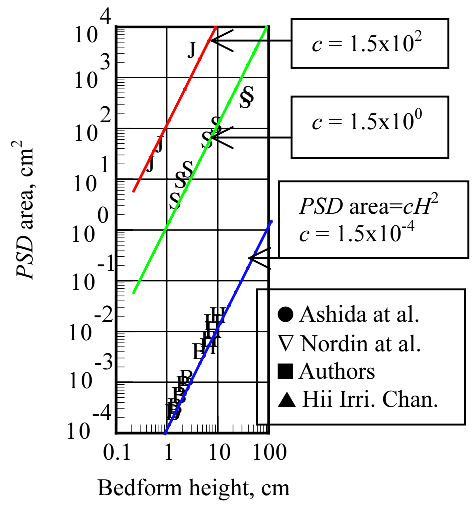

Figure 4: Functional relationship between spectrum and bedform height.

The area under wave number spectrum density function of ocean waves has a functional relationship with the second power of the significant wave height (Ochi, 1998). Similar to that, an attempt was made (1999) to find a relationship between power spectrum and bedform height. The auto-correlation function $R(\tau)$ of longitudinal bed elevation for lag distance τ with zero value is simply the mean square displacement of bed elevation. For bed elevation $Y(x)$ and longitudinal distance x, auto-correlation function with lag distance $\tau=0$ is given by

$$R(0) = \int_{-\alpha}^{\alpha} S(k)dk = E\left[Y^2\right] \qquad (1)$$

Here $S(k)$ = power spectrum density (*PSD*) function, k = wave number cycle/cm. Jain et al. (1974) assumed a certain range of wave numbers k_1 to k_n for fully developed dune bed profiles, over which the mean square value of bed elevation might remain unchanged. Therefore, the area under the *PSD* function for equilibrium sub-range of wave number k_1 to k_n of the bed profile could be given by

$$\sum_{k_1}^{k_n} S(k_i)\Delta k = E\left[Y^2\right] \qquad (2)$$

Assuming that the mean square of dune bed elevation Y is proportional to square of the average bedform height H, Equation (2) becomes

$$\sum_{k_1}^{k_n} S(k_i)\Delta k \propto H^2 \qquad (3)$$

or,
$$\sum_{k_1}^{k_n} S(k_i)\Delta k = cH^2 \qquad (4)$$

Here c is a proportional factor. If Equation (3) is multiplied by the constant 1/8ρg, then the potential energy of the sand wave profile is obtained. Therefore, Equation (3) gives the validity to the interpretation of wave number *PSD* function $S(k)$ of longitudinal bed profile as energy spectrum (Kinsman 1984).

The relationship between the *PSD* area and bedform height is verified in Figure 4 by our experimental and the Japanese Hii river irrigation channel data, along with data from Nordin et al. (1966), Ashida et al. (1967). In every case, Figure 4 shows that the *PSD* area is related with the 2nd power of average bedform height, but with a different proportional factor c because of different scales of the spectrum ordinate. On the other hand, the proportional factor for our data is 1.5X10^{-4}.

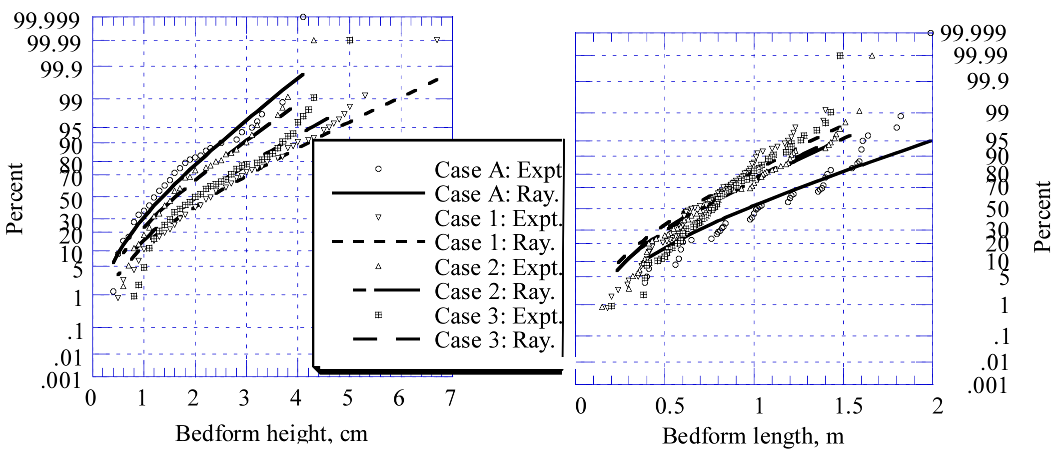

Figure 5: Rayleigh distribution of bedform height and bedform length.

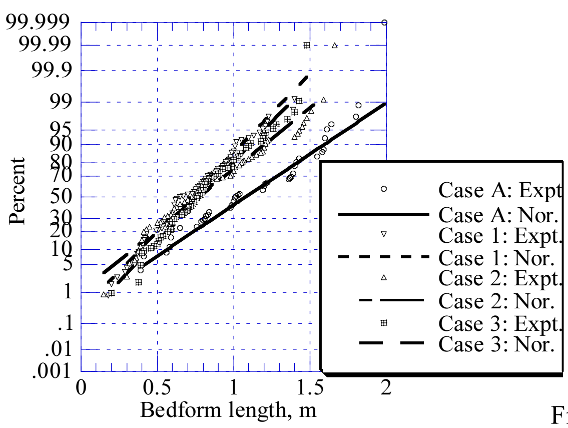

Figure 6: Normal dist. of bedform length.

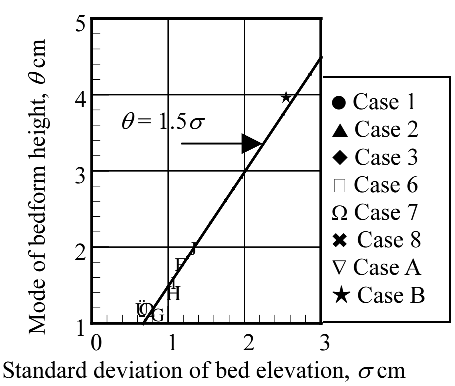

Figure 7: Relation between mode of bedform height and standard deviation of bed elevation.

Ashida et al. (1967) approached the probability distribution of dimensionless bedform heights and lengths, where experimental results of both the bedform features in the lower regime fitted the Rayleigh distribution well. It had been shown in an earlier study by the authors (1999) of groin bedforms that the bedform heights agreed with the Rayleigh distribution but the bedform length deviated from that distribution, especially for larger and smaller wavelengths. The distribution of bedform lengths rather fitted Normal distribution. The Rayleigh distributions of the bedform heights and lengths are shown in Figure 5. The bedform height distribution has a deviation from one experiment to another with respect to the parameter mode θ of the respective run. The standard deviation of bed elevation σ of each experiment has a relation (Figure 7) with the mode θ, which is given;

$$\theta = 1.5\sigma \qquad (5)$$

On the other hand, straight and dotted lines of Figure 6 indicate that the bedform length better has fitted Normal distribution, where the parameters mean and standard deviation are estimated from experimental data.

Nordin et al. (1966) showed that the significant sand wave height $H_{1/3}$, which means average of one-third highest bedform height, was equal to 3 times the standard deviation of

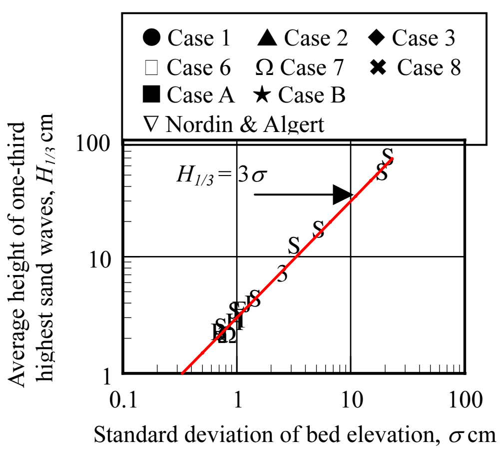

Figure 8: Relation between significant wave height and standard deviation of bed elevation.

bed elevation without considering the effects of hydraulic structure. The present analysis shows (Figure 8) that even in the cases of hydraulic structure beds, the $H_{1/3}$ is equal to 3 times the standard deviation of bed elevation. In a similar way to the phenomena of bedform without groin, bedform height in the presence of groins also increases with the increase of tractive force. During very large tractive force at the present of groins this relation might be different.

5 EQUIVALENT ROUGHNESS

Equivalent roughness of the experimental beds is computed by the resistance Equation (6) of hydraulic rough flow.

$$\frac{\overline{U}}{u_*} = 5.75 \log\left(\frac{R}{Ks}\right) + 6 \qquad (6)$$

Here $\overline{U}$ is mean velocity; u_* is bed shear velocity; Ks is equivalent roughness; R is hydraulic radius. As the side-wall of the flume is smooth and width-depth ratio is larger than five (Rijn, 1982), we do not use side-wall correction. Table 1 shows that the presence of groins effected the flow resistance. Case 1 groin bed has highest equivalent roughness among the groin-related experiments. On the other hand, the Case A experiences the lowest equivalent roughness. By analogy with the bedform analysis, equivalent roughness is also influenced by the groin interval, angle, height, and permeability. Among these factors, groin height and permeability cause most significant impact on the flume bed roughness (Table 1). The larger groin height of Case 4 causes higher equivalent roughness in the main channel than the lower groin height of Case 6.

The relative roughness, Ks/H ratio, of the experimental beds, which is (Yalin, 1977) a function of bedform steepness, is plotted in Figure 9 along with the bedform roughness methods predicted by the investigators. Even though the equivalent roughness of the groin experimental beds varies from one bed to another, the relative roughness, the Ks/H ratio, has only little variation from Case A bed. A close consistency of the relative roughness indicates the basic similarity of the groin beds configuration to the bed without groins even with different arrangement of groins for relatively low groin height and tractive force.

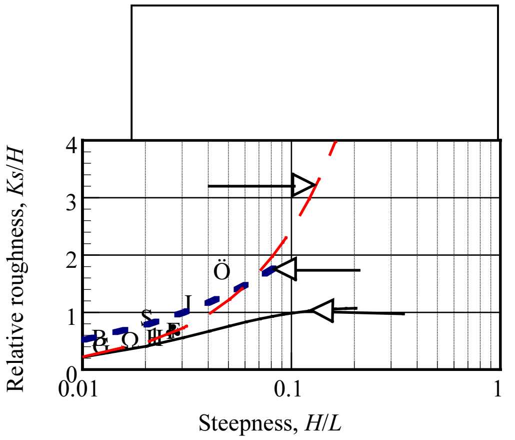

Figure 9: Comparison of bedform roughness.

6 CONCLUSION

Spectral peaks at higher wave-number of groin beds show more irregularities of sand waves compared to the bed without groin under the same hydraulic conditions. Because of the 3-dimension shape of sand waves, the bedform length of the groin bed measured by zero-crossing method varies from that of the slope change method. For relatively low groin height, bedform and relative roughness of groin bed are very similar to that of bed without groins.

The bedform features, bedform height and length follow separate distribution functions, Rayleigh distribution and Normal distribution respectively. The Rayleigh distribution parameter mode of bedform height has a functional relationship with standard deviation of bed elevation. By analogy with significant ocean waves, the area under the power spectrum density function of sand wave is related to the second power of average bedform height.

REFERENCES

Ashida, K. and Tanaka, Y., “A statistical study of sand waves,” Proc. 12th Congr. Int. Assn. for Hyd. Res., Ft. Collins, 2, pp.103-110, 1967.

Bahar, S. M. H., and Fukuoka, S., “The influence of submersible groins in series on bed geometry,” Ann. J. Hydr. Engrg, JSCE, vol. 43, pp. 671-676, 1999.

Bahar, S. M. H., “Change in bedform due to the installation of various hydraulic structures,” Master of Engrg. thesis, Hiroshima Univ., Japan, March, 1999.

Crickmore, M. J., “Effect of flume width on bedform characteristics,” Proc. ASCE, 96(HY2), pp.473-496, Feb. 1970.

Fukuoka, S., Nishimura, T., Okanobu, M. and Kawaguchi, H., “Flow and bed topography around groins installed in a straight channel,” Ann. J. Hydr. Engrg, JSCE, vol. 42, pp. 997-1002, 1998. (in Japanese).

Hino, M., “Equilibrium-range spectra of sand waves formed by flowing water,” J. Fluid Mech. 34, part 3, pp.565-573, 1968.

JSCE Task Committee, “The bed configuration and roughness of alluvial streams,” Committee on Hydr. and Hydr. Engineering, JSCE, 1974

Jain, S. C. and Kennedy, J. F., “The spectral evolution of sedimentary bed forms,” J. Fluid Mech. 63, 2, .301-314, 1974.

Kinsman, B., “Wind waves: Their generation and propagation on the ocean surface,” Dover Publications, Inc., 1984.

Nordin, C. F., and Algert, J. H., “Spectral analysis of sand waves,” Proc. ASCE, 92(HY5), pp.95-114, Sept. 1966.

Ochi, M. K., “Ocean waves: The stochastic approach,” Cambridge Uni. Press, 1998.

Shinohara, K., and Tsubaki, T., “On the characteristics of sand waves formed upon the beds of the open channels and rivers,” Rep. of Res. Inst. for appl. Mech., Vol. VII, No. 25, Kyushu Uni., Kyushu, Japan 1959.

Swart, D. H., “Predictive equations regarding coastal transport,” Proc., 15th Coastal Engrg. Congr., Vol. II, Chapter 66, Honolulu, Hi., 1976, pp. 1113-1133.

Van Rijn, L. C., “Equivalent roughness of alluvial bed,” J. Hydr. Engrg., ASCE, 108(10), pp.215-1218, 1982.

Yalin, M. S., “Mechanics of sediment transport,” Pergamon Press Ltd, 1977.